Electronic Supplementary Material (ESI) for Inorganic Chemistry Frontiers.

Supporting Information

Porous High-Entropy Oxides Nanosheets as Highly-efficient Electrocatalyst for Water Oxidation

Ting Huang[1], Cui Gao[1], Yun Tong[2]* and Xiuli Lu[1]*

[1] MOE International Joint Laboratory of Materials Microstructure, Institute for New Energy Materials and Low Carbon Technologies, School of Material Science & Engineering, Tianjin University of Technology, Tianjin 300384, China. (E-mail: luxiuli@email.tjut.edu.cn)

[2] School of Chemistry and Chemical Engineering, Key Laboratory of Surface & Interface Science of Polymer Materials of Zhejiang Province, Zhejiang Sci-Tech University, Hangzhou 310018, Zhejiang, China. (Email: tongyun@mail.ustc.edu.cn)

Table of contents

Experimental Section

Chemicals

Chromic(III) chloride hexahydrate ($CrCl_3 \cdot 6H_2O$, AR), iron(III) chloride hexahydrate ($FeCl_3 \cdot 6H_2O$, AR), cobalt chloride hexahydrate ($CoCl_2 \cdot 6H_2O$, AR), nickel(II) chloride hexahydrate ($NiCl_2 \cdot 6H_2O$, AR), manganese(II) chloride tetrahydrate ($MnCl_2 \cdot 4H_2O$, AR) and magnesium chloride hexahydrate($MgCl_2 \cdot 6H_2O$, AR) were purchased from Aladdin. Zinc chloride ($ZnCl_2$, ≥98%) was purchased from Alfa Aesar. Dicyanamide ($C_2H_4N_4$, AR) and ammonium chloride (NH_4Cl, AR) were purchased from Sinopharm Chemical Reagent Co. Ltd. Potassium hydroxide (KOH, ≥85 %) and ethanol (C_2H_5OH, 99.99%) were purchased from Shanghai Fuchen Chemical Reagent Co., LTD. Nafion 117 solution (5 %) was purchased from Sigma-Aldrich. Ultrapure water with a resistivity of 18.2 MΩ cm made from a Milli-Q water purification system was used in this work. Unless otherwise noted, all solvents and pharmaceuticals are commercially available and can be used directly.

Preparation of high-entropy catalysts

The $(FeCoNiCrZn)_3O_4$ HESO was synthesized by low temperature template sintering method. Firstly, (FeCoNiCrZn)O-CN nanosheet was preparated. In detial, 5 g NH_4Cl and 1 g $C_2H_4N_4$ were dissolved in 20 mL deionized water at 50 ºC under sustained stirring and cooled down to room temperature (named as solution A). In addition, the equimolar $FeCl_3 \cdot 6\ H_2O$, $CoCl_2 \cdot 6H_2O$, $NiCl_2 \cdot 6H_2O$, $CrCl_3 \cdot 6H_2O$ and $ZnCl_2$ (total metal salts of 0.91 mmol) and 16.7 g NH_4Cl was dissolved in 100 mL deionized water under continuously stirring (named as solution B). Then, 10 mL of solution B was mixed with 20 mL of solution A. Following that, the mixed solution was vigorously stirred for 30 minutes to obtain a homogeneous solution at room temperature, and named as solution C. The solution C was exposed to freeze-drying in a freeze dryer with a vacuum for 48 h. Finally, the freeze-dried power was placed in a covered crucible under air and heated at 550 ºC for 4 h with a heating rate of 3 ºC /min in a muffle furnace to obtain (FeCoNiCrZn)O-CN nanosheet.

The $(FeCoNiCrZn)_3O_4$ HESO nanosheet was synthesized from the precursor of (FeCoNiCrZn)O-CN nanosheet. Briefly, the resultant (FeCoNiCrZn)O-CN was milled into a power in a mortar. Then, the (FeCoNiCrZn)O-CN power was transferred into a crucible and heated at 550 ºC for 1 h at a rate of 3 ºC /min in a muffle furnace. As a result, the $(FeCoNiCrZn)_3O_4$ HESO nanosheets were obtained. Quaternary metal oxide $(FeCoNiCr)_3O_4$ and quinary metal oxides ($(FeCoNiCrM)_3O_4$, where M is Mn or Mg) were prepared using the same method using the corresponding as-synthesized metal hydrochloride templates.

Characterizations of materials

The morphology of the samples was characterized by transmission electron microscopy (TEM) microscope with a LaB6 Gun (Tecnai G2 Spirit TWIN, FEI, America) and the microstructure and element mapping of the samples were characterized by Tecnai G2 F20 High-resolution transmission electron microscopy (HRTEM) produced by FEI Company of the United States. The composition of the samples was analyzed using energy dispersive spectroscopy (EDS) equipped in the TEM. The structure of the as-prepared samples was characterized by X-ray diffraction (XRD) (SmartLab 9 KW, Rigaku, Japan) with Cu Kα radiation (λ = 1.54178 Å). X-ray photoelectron spectra (XPS, ESCALAB 250 Xi spectrometer, Thermo Scientific, America) with an Al Kα as the excitation source was used to investigate the energies of the elements on the surface and the binding energy of C 1s was fixedat 284.8 eV to correct the XPS spectrum.

Electrochemical measurements of catalysts for OER

The electrochemical measurements of as-prepared samples were carried out in a standard three electrode cell system connected to an electrochemical workstation (CHI 760E, Shanghai Chenhua) in 100 mL 1.0 mol/L KOH in the air atmosphereat and at room temperature (25 °C). A graphite rod was used as the counter electrode, an Ag/AgCl electrode was used as the reference electrode and glassy carbon electrode (GCE) with diameter of 3 mm coated with catalysts was used as working electrode.

The area of the GCE was calculated to be 0.0707 cm^2 , which was used to determine the current density in the linear scan voltammetry (LSV). Before each measurement, the GC electrode was polished with alumina powder and rinsed thoroughly with deionized water and ethanol to avoid any contamination from previous measurements. For the preparation of the working electrode, 3 mg catalyst was ultrasonically dispersed into a solution consisting of 960 μL of ethanol, 2 mg carbon power (Vulcan XC 72) and 40 μL of Nafion solution (5 wt%). 10 μL of the formed catalyst slurry dropped onto the GC electrode and allowed to dry naturally under ambient conditions. The mass loading was 0.85 mg/cm^2 .

Before OER measurements, 20 cycles of cyclic voltammetry activation were conducted in a potential range from 1.2 to 1.8 V versus RHE at a scan rate of 100 mV/s to obtain stable polarization curves without iR-compensation. All potentials in this work were calibrated to reversible hydrogen electrode (RHE) according to the Nernst equation: $E_{RHE} = E_{Ag/AgCl} + 0.059 \times pH + 0.204$. The Tafel slopes were calculated according to $\eta = a + b\log j$, where b, η , and j are attributed to the Tafel slope, overpotential, and current density, respectively. Electrochemical impedance spectroscopy (EIS) is performed at the potential corresponding to 10 mA/cm^2 within a frequency range of 0.01-1000,000 Hz with a 5 mV AC amplitude. Electrochemical impedance spectroscopy (EIS) was measured at 5 mV from 1000,000 to 0.01 Hz. To determine the ECSAs of the as-prepared catalysts, double layer capacitance (C_{dl}) was determined from the cyclic voltammetry curves recorded at different scan rates (10, 15, 20, 25, and 30 mV/s) in the non-Faradaic potential range of 0.95-1.05 V versus RHE. The C_{dl} was obtained by plotting $\Delta J = (J_a - J_c)/2$ at 1.0 V versus RHE against the scan rates, where J_a and J_c are the anodic and cathodic current densities, respectively. The ECSA was estimated following the equation: $ECSA = C_{dl}/C_s$, where C_s is the specific capacitance and is 40 $\mu F/cm^2$ according to the literature. Faradaic efficiency (FE) is determined using the formula: $FE=V_e/V_t$. The V_e reflects the experimental volume of the generated O_2 gas, and V_t denotes the calculated volume of O_2 gas, determined by the formula: $V_t = V_mQ/nF$, where V_m (the molar volume of the ideal gas) is defined as 22.4 L/mol, Q is the electric charge quantity and n (the number

of electrons transfer) is 4 for OER. The long term stability of the as-prepared catalysts was evaluated by the chronoamperometry method. All electrochemical results are presented without IR compensation.

The details of in-situ Raman spectroscopy

The Raman spectra were taken on a high-resolution laser confocal fiber Raman spectrometer (HORIBA EVOLVTION, HORIBA Jobinyvon, France).The wavelength of the laser excitation source was 532 nm with a power of ~0.5 mW at a grating of 800 mm, and test wavelength 300-1200 cm^{-1}. Raman signals were recorded in-situ at OCP and under different applied potentials spanning from 1.1 V to 1.5 V vs RHE.

The details of in-situ FT-IR spectroscopy

ATR-SEIRAS was conducted using the ThermoFisher Nicolet iS50. An ultrathin Au layer was chemically deposited on the flat surface of a cylindrical silicon prism. The catalyst ink preparation method was the same as in electrochemical measurements. 100 μL of the catalyst ink solution was loaded on the gold-plated Si prism by drop-cast and dried under ambient conditions. The FTIR tests were conducted in a glassy four-necked electrolysis cell in 1 M KOH. The FTIR spectra were collected in the potential range from OCP to 1.70 V with an interval of 50 mV under OER reaction conditions.

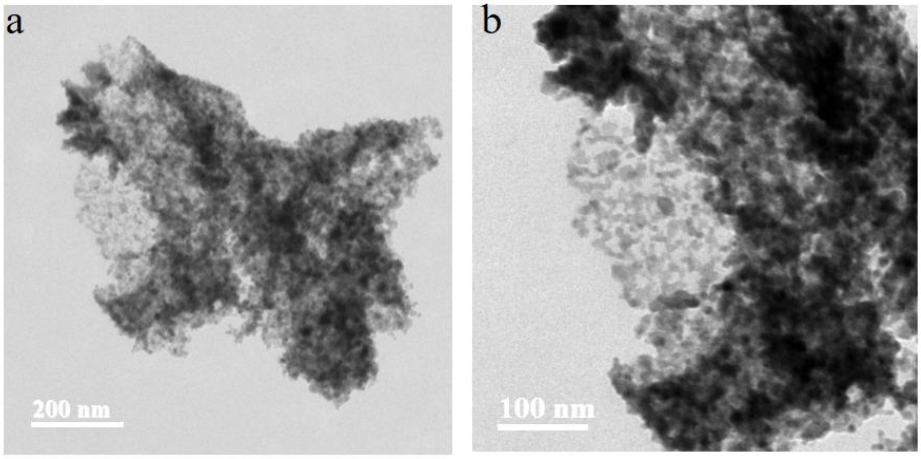

Figure S1. The TEM images of $(FeCoNiCrMn)_3O_4$ sample.

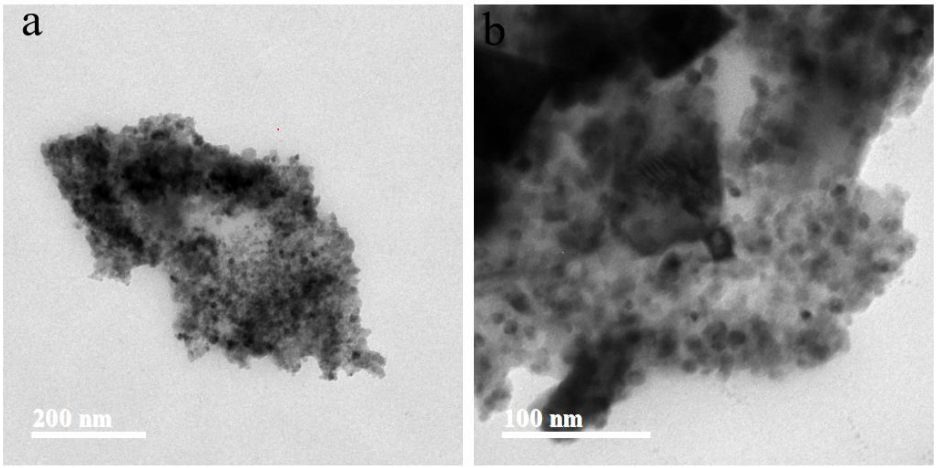

Figure S2. The TEM images of $(FeCoNiCrMg)_3O_4$ sample.

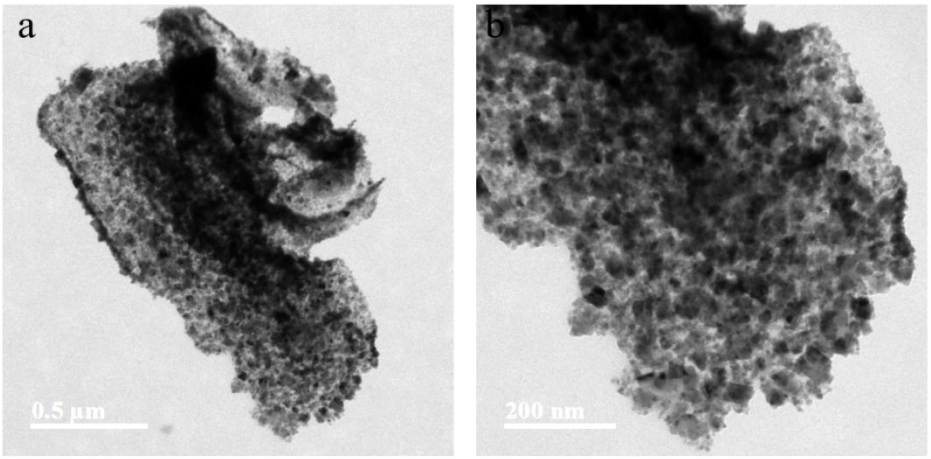

Figure S3. The TEM images of $(FeCoNiCr)_3O_4$ sample.

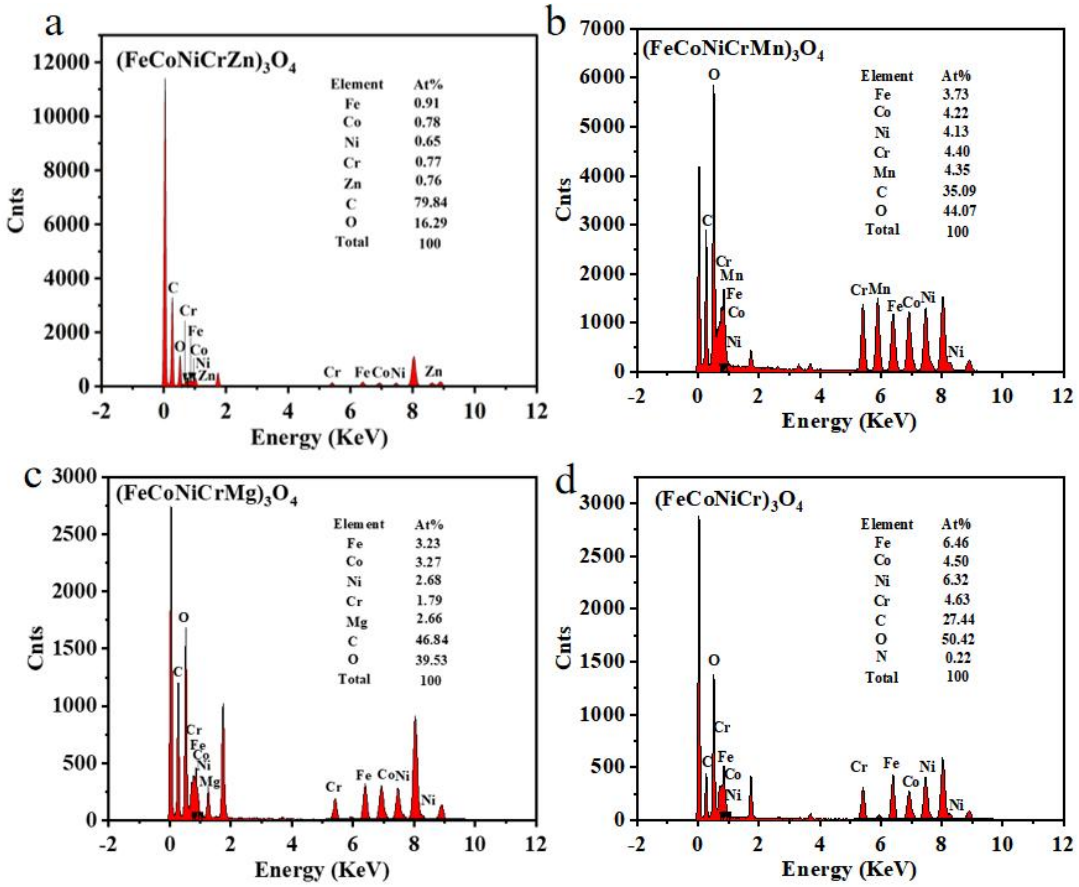

Figure S4. EDS spectra and corresponding atomic contents of each elements for (a) $(FeCoNiCrZn)_3O_4$, (b) $(FeCoNiCrMn)_3O_4$, (c) $(FeCoNiCrMg)_3O_4$ and (d) $(FeCoNiCr)_3O_4$.

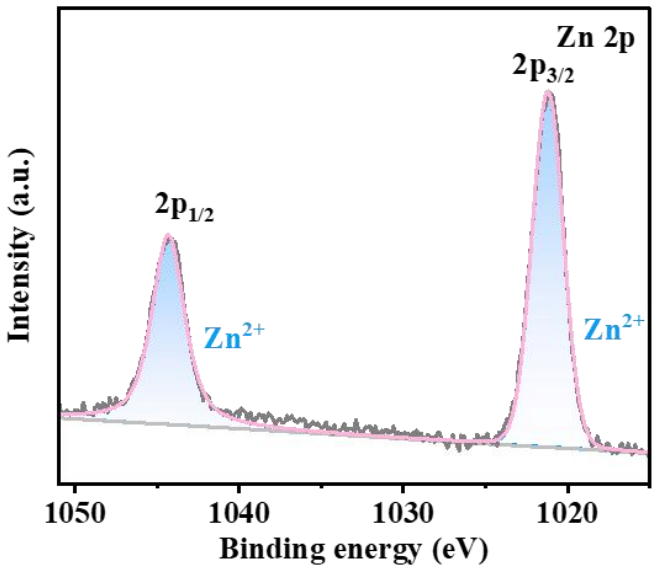

Figure S5. XPS spectrum of Zn 2p for the $(FeCoNiCrZn)_3O_4$ sample.

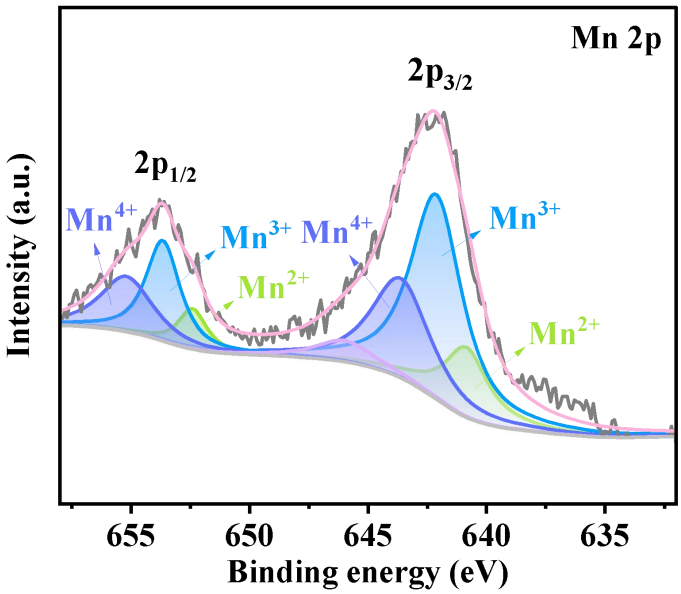

Figure S6. XPS spectrum of Mn 2p for the $(FeCoNiCrMn)_3O_4$ sample.

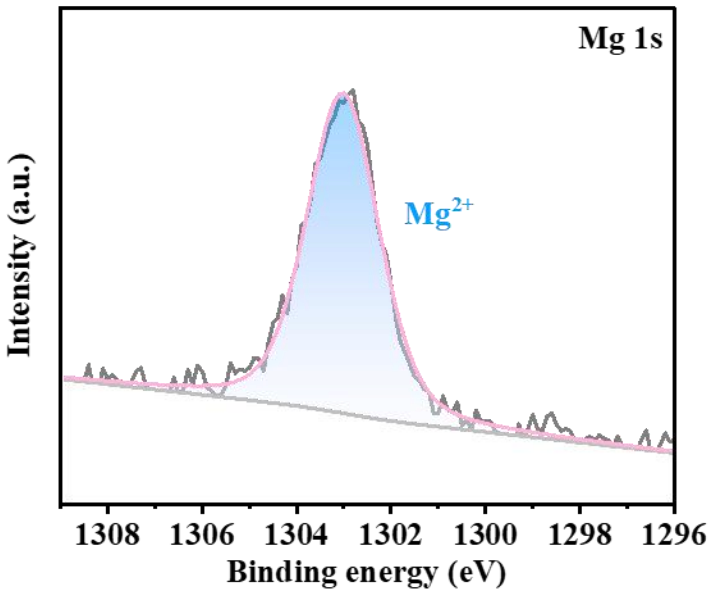

Figure S7. XPS spectrum of Mg 1s for the $(FeCoNiCrMg)_3O_4$ sample.

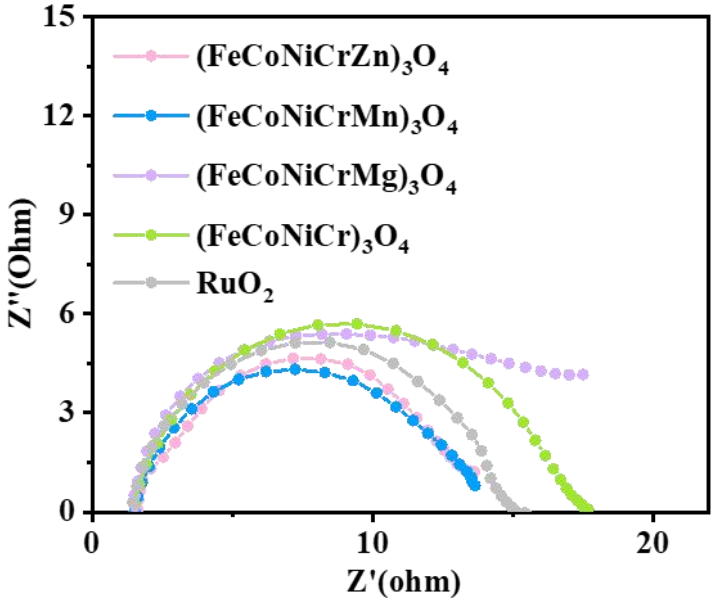

Figure S8. The EIS spectra of the obtained various high-entropy oxides and RuO_2.

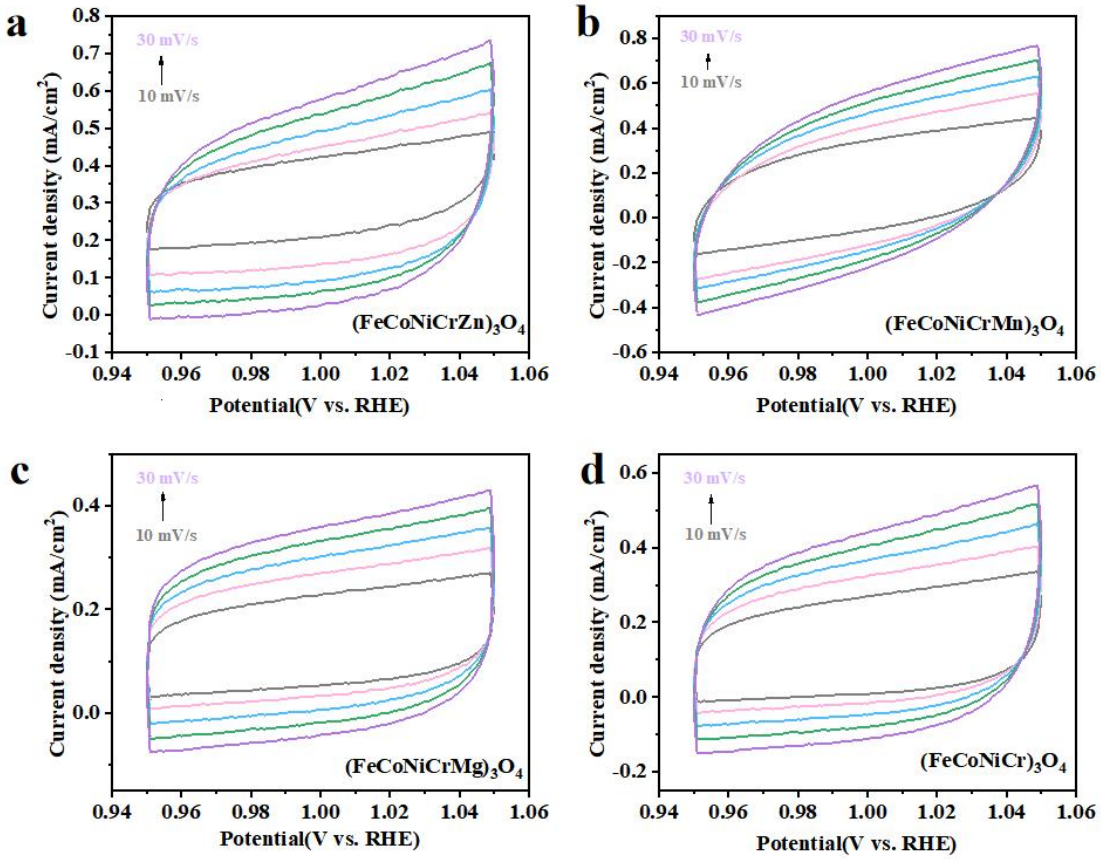

Figure S9. The CV curves of (a-d) $(FeCoNiCrZn)_3O_4$, $(FeCoNiCrMn)_3O_4$, $(FeCoNiCrMg)_3O_4$ and $(FeCoNiCr)_3O_4$ samples at scan rates of 10 to 30 mV s^{-1}.

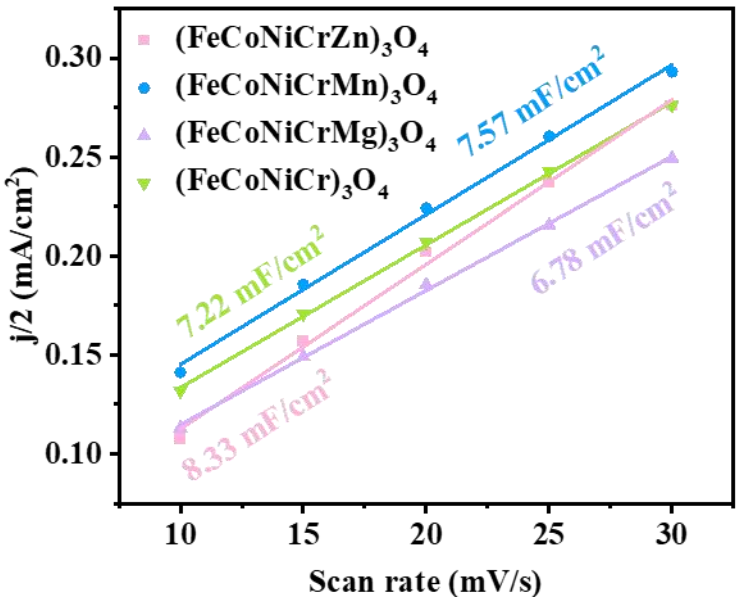

Figure S10. The fitting C_{dl} values of the obtained various high-entropy oxides.

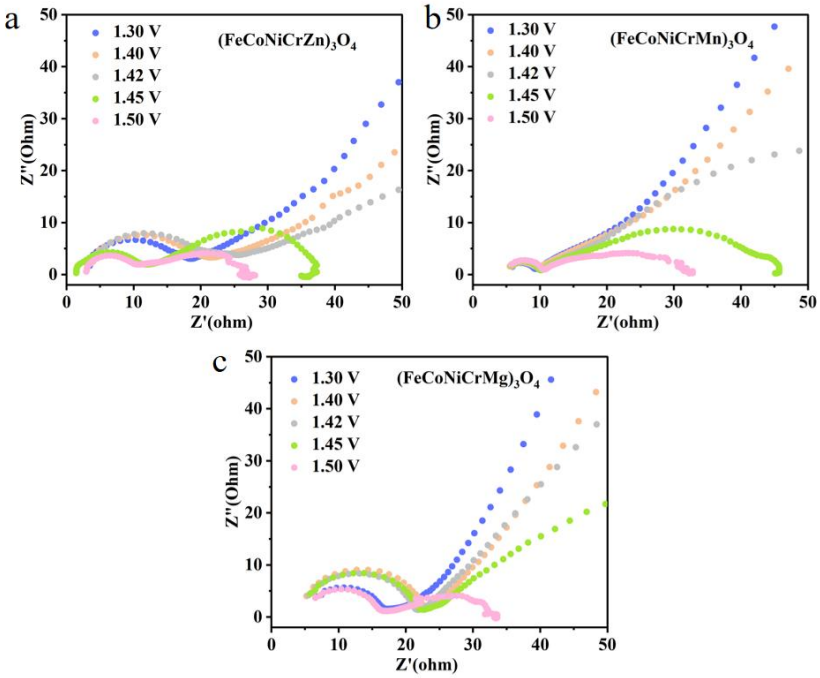

Figure S11. The Nyquist plots of (a) $(FeCoNiCrZn)_3O_4$, (b) $(FeCoNiCrMn)_3O_4$ and (c) $(FeCoNiCrMg)_3O_4$ at different potentials.

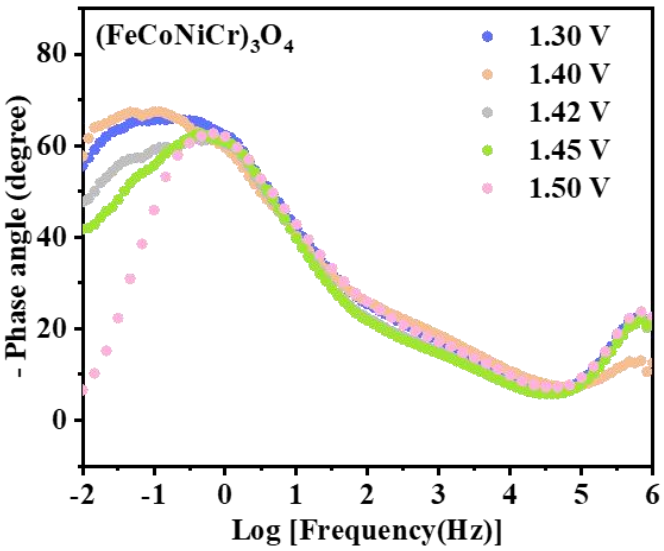

Figure S12. The Bode phase plots of $(FeCoNiCr)_3O_4$ sample.

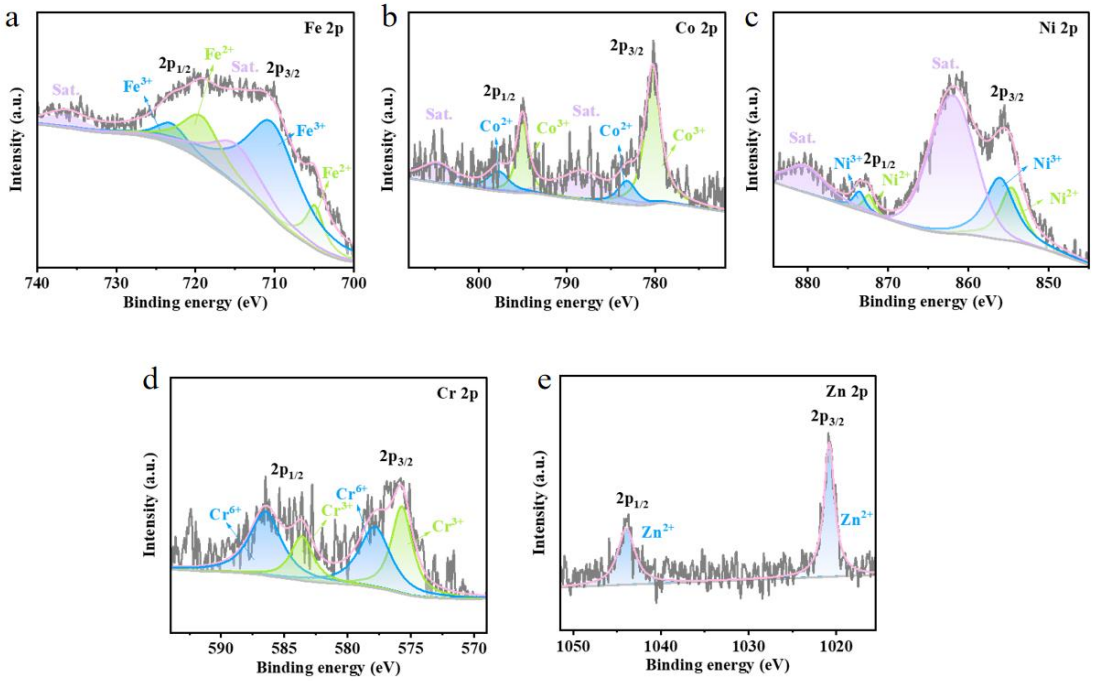

Figure S13. The XPS spectra of $(FeCoNiCrZn)_3O_4$ after OER test, (a) Fe 2p, (b) Co 2p, (c) Ni 2p, (d) Cr 2p and (e) Zn 2p.

Table S1. The contents of each metals in the prepared high-entropy oxides by ICP-MS test.

Samples	Fe(at%)	Co(at%)	Ni(at%)	Cr(at%)	Zn(at%)/ Mn(at%)
$(FeCoNiCrZn)_3O_4$	19.0	22.4	20.3	19.5	18.8
$(FeCoNiCrMn)_3O_4$	25.3	18.8	17.8	17.7	20.4
$(FeCoNiCr)_3O_4$	26.4	22.7	27.0	23.9	-

Table S2. The elemental contents of the prepared high-entropy oxides by EDS result.

Samples	Fe(at%)	Co(at%)	Ni(at%)	Cr(at%)	Zn(at%)/ Mn(at%)/ Mg(at%)
$(FeCoNiCrZn)_3O_4$	0.91	0.78	0.65	0.77	0.76
$(FeCoNiCrMn)_3O_4$	3.73	4.22	4.13	4.40	4.35
$(FeCoNiCrMg)_3O_4$	3.23	3.27	2.68	1.79	2.66
$(FeCoNiCr)_3O_4$	6.46	4.50	6.32	4.63	-

Table S3. The XPS data of each element for the high-entropy oxides.

Elements	$(FeCoNiCr)_3O_4$ $2p_{3/2}/2p_{1/2}$	$(FeCoNiCrZn)_3O_4$ $2p_{3/2}/2p_{1/2}$	$(FeCoNiCrMn)_3O_4$ $2p_{3/2}/2p_{1/2}$	$(FeCoNiCrMg)_3O_4$ $2p_{3/2}/2p_{1/2}$
Fe^{2+}	710.15/723.19	710.36/723.52	710.35/723.27	710.56/723.80
Fe^{3+}	712.54/725.44	712.29/725.41	712.93/725.04	712.94/725.85
Co^{2+}	781.91/796.65	781.59/796.39	781.97/797.09	781.96/796.61
Co^{3+}	779.93/795.01	780.15/795.12	780.06/795.32	780.29/795.34
Ni^{2+}	854.43/872.37	854.70/871.85	854.57/871.88	854.85/872.51
Ni^{3+}	855.81/874.72	856.12/872.92	856.10/872.95	856.40/874.49
Cr^{3+}	576.39/586.06	576.12/584.86	576.14/585.85	576.36/586.01
Cr^{6+}	579.23/588.24	578.24/586.58	578.78/588.07	579.30/588.24
O_I	530.11	530.00	529.93	530.12
O_{II}	532.61	531.85	531.52	531.35
O_{III}	533.21	533.47	533.54	533.41
Zn^{2+}	-	1021.21/1044.32	-	-
Mg^{2+}	-	-	-	1303.02 (1 s)
Mn^{2+}	-	-	641.64/652.45	-
Mn^{3+}	-	-	641.84/653.68	-
Mn^{4+}	-	-	643.47/655.22	-

Table S4. The ratios of high- and low-valence states of each elements.

Samples	Fe^{3+}/ Fe^{2+}	Co^{3+}/Co^{2+}	Ni^{3+}/Ni^{2+}	Cr^{6+}/Cr^{3+}
$(FeCoNiCrZn)_3O_4$	2.10	2.73	1.12	0.44
$(FeCoNiCrMn)_3O_4$	1.38	1.89	1.06	0.64
$(FeCoNiCrMg)_3O_4$	1.06	1.62	1.02	1.14
$(FeCoNiCr)_3O_4$	0.93	0.89	0.97	0.67

Table S5. Overpotential and stability of metal oxides reported in this paper and literature at current density of 10 mA cm^{-2}.

Catalysts	Substrate	Overpotential at 10 mA/cm^2 (mV)	stability	Ref.
$(FeCoNiCrZn)_3O_4$	GCE	216	15	This work
CoP-TiO_x	GCE	337	8	[1]
HEO/MWCNT	GCE	351	12	[2]
4%Te-$NiCo_2O_4$	GCE	338	19	[3]
$Pr_{0.5}Sr_{0.5}Co_{0.8}Fe_{0.2}O_{3-\delta}$	GCE	320	10	[4]
$K_{0.8}Na_{0.2}(MgMnFeCoNi)F_3$	GCE	314	10	[5]
$CoFe_2O_4$ NSs	GCE	275	10	[6]
La-HEO@NiFeOOH	carbon cloth	262	30	[7]
FeCoNiRu HEA	GCE	243	40	[8]
Co_9S_8@NiFe LDH	GCE	220	20	[9]
CoNiCuMnAl@C	GCE	215	24	[10]
$Ir_{88}Ru_{12}$@CM	GCE	210	24	[11]
$NiFe(OH)_x/(Ni, Fe)Se_2$	GCE	180	20	[12]

Table S6. The comparison of XPS result before and after OER test.

Samples	**Fe^{3+}/ Fe^{2+}**	**Co^{3+}/Co^{2+}**	**Ni^{3+}/Ni^{2+}**	**Cr^{6+}/Cr^{3+}**	**O_v**
$(FeCoNiCrZn)_3O_4$	2.10	2.73	1.12	0.44	22.8%
$(FeCoNiCrZn)_3O_4$-post OER	2.25	3.23	0.92	1.40	64.8%

References:

[1] Z. Liang, W. Zhou, S. Gao, R. Zhao, H. Zhang, Y. Tang, J. Cheng, T. Qiu, B. Zhu, C. Qu, W. Guo, Q. Wang, R. Zou, *Small* **2019**, *16*.

[2] D. Wang, Z. Liu, S. Du, Y. Zhang, H. Li, Z. Xiao, W. Chen, R. Chen, Y. Wang, Y. Zou, S. Wang, *J. Mater. Chem. A.* **2019**, *7*, 24211-24216.

[3] S. F. Li, X. Li, D. Yan, *Chem. Commun.* **2023**, *59*, 8834-8837.

[4] S. Wu, J. Li, J. Hu, Y. Huang, H.-S. Xu, K. Tang, *ACS Appl. Energy Mater.* **2023**, *6*, 6289-6298.

[5] T. Wang, H. Chen, Z. Z. Yang, J. Y. Liang, S. Dai, *J. Am. Chem. Soc.* **2020**, *142*, 4550-4554.

[6] H. Fang, T. Huang, D. Liang, M. Qiu, Y. Sun, S. Yao, J. Yu, M. M. Dinesh, Z. Guo, Y. Xia, S. Mao, *J. Mater. Chem. A.* **2019**, *7*, 7328-7332.

[7] Z. Wang, S. Han, Y. Zhang, Y. Wang, *Fuel* **2024**, *357*.

[8] K. Huang, J. Xia, Y. Lu, B. Zhang, W. Shi, X. Cao, X. Zhang, L. M. Woods, C. Han, C. Chen, T. Wang, J. Wu, Y. Huang, *Adv. Sci.* **2023**, *10*, e2300094.

[9] X. Feng, Q. Jiao, Z. Dai, Y. Dang, S. L. Suib, J. Zhang, Y. Zhao, H. Li, C. Feng, A. Li, *J. Mater. Chem. A.* **2021**, *9*, 12244-12254.

[10] S. Wang, W. Huo, F. Fang, Z. Xie, J. K. Shang, J. Jiang, *Chem. Eng. J.* **2022**, *429*.

[11] T. B. N. Huynh, J. Song, H. E. Bae, Y. Kim, M. D. Dickey, Y. E. Sung, M. J. Kim, O. J. Kwon, *Adv. Funct. Mater.* **2023**, *33*.

[12] C. Liu, Y. Han, L. Yao, L. Liang, J. He, Q. Hao, J. Zhang, Y. Li, H. Liu, *Small* **2021**, *17*, e2007334.